

Original Article

SECONDARY METABOLITES FROM RICE CULTURE OF *ASPERGILLUS* SP. ISOLATED FROM *MELALEUCA SUBULATA* (CHEEL) CRAVEN LEAVES AND THEIR ANTICANCER ACTIVITY

HAITHAM ALI IBRAHIM¹, REHAM RAGAEI IBRAHIM¹, REEM ALAA KAMEL², SHAHENDA METWALLY EL-MESSERY³, FATMA ABDELKADER MOHARRAM^{1*}

¹Pharmacognosy Department, Faculty of Pharmacy, Helwan University, ²Mansheyat El-Bakry, General Hospital, Heliopolis, ³Department of Pharmaceutical Organic Chemistry, Faculty of Pharmacy, Mansoura University
Email: famoharram1@hotmail.com

Received: 17 Jun 2020, Revised and Accepted: 27 Aug 2020

ABSTRACT

Objective: *Aspergillus* fungus is a rich source of natural products with broad biological activities. This study was conducted to identify secondary metabolites from the rice culture of *Aspergillus* species isolated from *Melaleuca subulata* leaves and evaluated their anticancer activity.

Methods: Ethyl acetate extract was fractionated on silica gel and Sephadex columns. Structures of the compounds were established using physical and chemical methods. Cytotoxic activities of the extract and pure compounds against two human cancer cell lines (Mcf-7 and Hep G2) were evaluated using microculture tetrazolium assay as well as the mode of the cytotoxicity was evaluated. Molecular docking studies have been performed using the Hsp 90 enzyme as an anticancer target.

Results: Methyl linoleate (1), arugosin C (2), ergosterol (3), sterigmatocystin (4), diorcinol (5), alternariol-5-*O*-methyl ether (6), averufin (7), averufanin (8), and alternariol (9) were identified from ethyl acetate extract. All tested compounds exhibit weak activity against MCF-7 and Hep G2 cell lines but a mixture of compounds 7 and 8 is considered to be more active towards both MCF-7 and Hep G 2 in comparison to other compounds. Compound 4 exhibits moderate activity against Hep G2 only as well as the ethyl acetate extract exerts moderate activity against MCF-7 cell line. Moreover, compound 4 and a mixture of 7 and 8 caused a decrease in the number of Hep G2 cancer cells due to apoptotic and necrotic processes. Most active anticancer candidates 7 and 8 showed binding to the active site similar to geldanamycin reference ligand.

Conclusion: Secondary metabolites identified from *Aspergillus* sp. and their anticancer activity were evaluated. Molecular docking suggested active candidates as Hsp 90 inhibitors.

Keywords: Anthraquinones, Apoptotic, *Aspergillus* sp, *Melaleuca subulata*, Necrotic, Xanthone

© 2020 The Authors. Published by Innovare Academic Sciences Pvt Ltd. This is an open access article under the CC BY license (<http://creativecommons.org/licenses/by/4.0/>)
DOI: <http://dx.doi.org/10.22159/ijpps.2020v12i10.38773>. Journal homepage: <https://innovareacademics.in/journals/index.php/ijpps>.

INTRODUCTION

Plant endophytes are considered as a fungal or bacterial microorganism that spends whole or part of its life in the living tissues of the plant without causing apparent symptoms of disease [1, 2]. Taxol, sanguinarine, and gallic acid are examples for secondary metabolites obtained from the endophytic fungi known to possess significant biological activities like anticancer, antimicrobial, and antioxidant activities [3-5]. Recently, a great deal of interest has been generated in the discovery of remarkable pharmacological agents from endophytic fungi [2]. Genus *Aspergillus* represents a large genus of fungi that includes about 185 species distributed worldwide with pathological and therapeutic importance [6]. Some of the secondary metabolites isolated from *Aspergillus* species are well known as penicillin, viridivatin, mevinolin, pseurotin A, and cyclopiazonic acid [6]. Particularly, secondary metabolites isolated from different *Aspergillus* species have frequently attracted the interest of pharmacologists due to their broad range of biological activities as anticancer and antimicrobial effects as well as their structural diversity range from polyketides, terpenoids, and alkaloids [6-10]. *M. subulata* (Cheel) Craven belongs to the family Myrtaceae and is cultivated in Egypt. This study aimed to investigate the metabolites from *Aspergillus* sp. isolated from leaf tissue of *M. subulata* and to evaluate the anticancer activity of the total ethyl acetate extract and the pure isolated compounds. Apoptotic and necrotic studies were done to detect the mode of cell death as well as molecular docking was applied to suggest the mechanism of anticancer activity of most active compounds.

MATERIALS AND METHODS

General

Column chromatography was carried out on silica gel 60 (Merck, Darmstadt, Germany) and Sephadex LH-20 (Sigma-Aldrich

Steinheim, Germany). Analytical and preparative TLC was performed on pre-coated silica gel 60 F₂₅₄ plates (Merck, Darmstadt, Germany). 1D and 2D NMR spectroscopic data of the isolated pure compounds were recorded on Bruker Avance [Bruker, Rheinstetten, Germany (400, 500 and 600 MHz for ¹H NMR and 100,125 and 150 for ¹³C NMR)]. Results were reported as δ ppm values relative to TMS as an internal reference. ESI-MS was done on a Micromass AC-TOF spectrometer (Micromass, Agilent Technologies 1200 series, Waldbronn, Germany). UV spectra were recorded on a UV-, V-630 BIO spectrophotometer (JASCO, USA). All other chemicals and solvents were of analytical grade. Human breast adenocarcinoma (MCF-7) and Hepatocellular carcinoma cells (Hep G2) were purchased from ATCC, VA, USA. Fetal bovine serum, L-glutamine, penicillin, streptomycin s, amphotericin B, trypsin/EDTA were purchased from Sigma/Aldrich, USA. Dulbecco's Minimum Essential Media (DMEM) was purchased from Cambrex BioScience (Copenhagen, Denmark).

Fungal material

Melaleuca subulata (Cheel) Craven (Myrtaceae) fresh leaves were collected from El Orman Botanical Garden, Giza, Egypt in February 2017. The plant was identified by Dr. Trease Labib, former specialist of plant taxonomy, El Orman Botanical Garden, Giza, Egypt. The voucher specimen (18-Msu-1-2017) was deposited at the herbarium of the Pharmacognosy Department, Helwan University, Helwan, Egypt. Leaves were cut into small pieces and washed with sterilized distilled water, then carefully, the surfaces were treated with 70% aqueous ethanol (2 min, two times) followed by rinsing with sterilized distilled water and dried. The outer surface was scratched with a sterile scalpel and the inner tissues were cleaved into 1 cm small segments and carefully placed onto potato dextrose agar (PDA) plates [200 g potato, 20 g glucose, and 15 g agar in purified

water [11]. After 3-6 w from the plate's incubation at 25 °C, the resulted colonies with different morphological characteristics were selected and transferred to fresh PDA media and refrigerated at 40 °C. Pure strains were isolated by repeated inoculation.

Identification of fungal cultures

The fungal isolates were identified by a partial sequence of large subunit ribosomal RNA (18S rDNA). The total genomic DNA of the endophytic fungus was extracted from *in vitro* culture using the ABT DNA mini extraction kit (Applied Biotechnology Co. Ltd, Egypt) and firmly following the guidelines. The nuclear ribosomal internal transcribed spacers (ITS rDNA) were amplified as single fragments by Polymerase Chain Reaction (PCR). A pair of primers, ITS1 (sequence: 50-TCC GTA GGT GAA CCT GCG G-3') and ITS4 (sequence: 50-TCC TCC GCT TAT TGA TAT GC-3') were mixed with Hot starTaq Master Mix Kit and DNA template in an I Cycler (Bio-Rad, Hercules, Ca) thermal cycle according to the following protocol: (1) initial denaturation 95 °C for 15 min to activate Hot StarTaq® DNA polymerase; (2) denaturation 95 °C, 1 min (3) annealing for 56°C for 0.5 min, (4) extension at 72°C for 1 min, (5) final extension of 72 °C for 10 min. Steps from 2-4 were repeated 35 times [11]. Each sample consists of 25 µl of Taq polymerase master mix, 3 µl of primers ITS 1 and ITS 4 (10 pmol/µl each), 3 µl of template DNA 19 µl of water. 20 µl from the PCR product was purified by loading onto agarose gel (2% agarose in TBA buffer, 5 µl of ethidium bromide 1 % m/v solution per 100 ml of gel) then subjected to electrophoresis at 70 V for 60 min. The band due to the PCR product (approximate size 550 bp), which was detected by UV fluorescence, was isolated from the gel slice using the Gen Elute™ Gel extraction kit according to the manufacturer's protocol. The corresponding ITS-rDNA sequence of each fungus was then used for similarity analysis using the Blast N algorithm against the public database at the National Centre for Biotechnology Information (NCBI; <http://www.ncbi.nlm.nih.gov>). The sequence data have been submitted to and deposited at Gen Bank (accession number of MH665645). The search result showed that the sequence was most similar to different types of *Aspergillus* sp as shown from the phylogenetic trees that were constructed using Molecular Evolutionary Genetics Analysis (MEGA) version 10.0.5. A voucher strain is kept at Microbial Chemistry Department, Genetic Engineering and Biotechnology Research Division, National Research Centre, Dokki-Giza, Egypt.

Cultivation

Mass growth of fungi was carried out by transferring fungi from PDA media and mix it with 5 ml sterile distilled water then inoculated into 100 ml of yeast/malt extract broth (10 g malt extract; 4 g yeast extract; 4 g glucose) at 25 °C for 3 d to be used as the seed culture. 5 ml of seed culture was grown on a solid autoclaved rice substrate medium (5X1000 ml Erlenmeyer flasks, each containing 100 g rice, and 150 ml distilled water) for 14 d at 25 °C under the static station.

Extraction and isolation of the secondary metabolites

300 ml of the ethyl acetate were added to the rice cultures and left overnight; then it was subjected to repeated extraction with ethyl acetate for 3-5 d till exhaustion, then the collected extract was evaporated under vacuum yielding 4.7 g of dry extract. The residue was dissolved in 40 ml of dichloromethane (DCM)/MeOH mixture (90:10 v/v), mixed with 15 g silica gel and dried at 40 °C. The dry residue was subjected to fractionation on a silica gel column (200 g, 60 x 3 cm) and eluted with cyclohexane then gradually increasing the polarity with DCM (20%, 40% till 100% DCM), followed by 1%, 3%, 5% till 50% MeOH/DCM to give 19 fractions each of 0.5 l. Based on their behavior under UV light and spraying reagents on TLC, they were collected into six major fractions (I-VI). Fr. I (1.1 g) was chromatographed on a silica gel column and eluted with cyclohexane: DCM in gradient order to yield a chromatographically pure sample of **1** (10 mg). Fr. II (0.4 g) was fractionated on a Sephadex LH-20 using DCM/MeOH (1:1v/v) as an eluent to afford two subfractions. The first subfraction was further purified on a Sephadex LH-20 column using DCM: MeOH (1:1v/v) as an eluent to give pure sample **2** (4.8 mg). Compound **3** (7.4 mg) was precipitated from the second subfraction by excess MeOH. Fr. IV (0.8 g) was precipitated from DCM by the addition of excess cyclohexane to give

a pure sample of **4** (8 mg). Fr. V (0.2 g) was subjected to Sephadex LH-20 column using DCM: MeOH (1:1v/v) to afford two subfractions. The first subfraction was further subjected to Sephadex column and eluted with DCM/MeOH (1: 1) to yield 6.5 mg of compound **5**. The second subfraction was applied to preparative TLC (PTLC) using DCM/MeOH (95: 5) followed by a Sephadex column to afford a pure sample of **6** (1.4 mg) and a mixture of **7** and **8** (4.5 mg). Fr. VI (0.3 g) was fractionated on a Sephadex LH-20 column and eluted with MeOH to give a chromatographically pure sample of **9** (0.8 mg). The purity of the isolated compounds was established based on their appearance under UV-light and behavior towards spray reagent on TLC.

Compound 1: Colorless oil; R_f (0.5, DCM: cyclohexane, 1:1); it gives intense violet color with anisaldehyde/sulfuric acid reagent. $^1\text{H NMR}$ (500 MHz, CDCl_3 -d): δ_{H} 5.29 (m, 4H, H-9,10,12,13), 3.60 (s, 1H, COOCH_3), 2.70 (t, 2H, $J = 6.5$ Hz, CH_2 -2), 2.23 (t like, 2H, $J = 7.5$ Hz, CH_2 -11), 1.96 (m, 2H, CH_2 -14), 1.55 (2H, m, CH_2 -3), 1.23; 1.18 (CH_2)_n, 0.81 (m, 3H, CH_3 -18).

Compound 2: Yellow powder; R_f (0.6, DCM/MeOH, 97:3); dark purple color with anisaldehyde/sulfuric acid reagent. UV (MeOH, λ_{max} , nm): 308; 358 (sh). $^1\text{H NMR}$ (500 MHz, CDCl_3 -d) and $^{13}\text{C NMR}$ (125 MHz, CDCl_3 -d) data (table 1); Positive ESI-MS: m/z : 447. 3 [M+Na]⁺.

Compound 3: White powder; R_f (0.31, DCM/MeOH, 97:3); it gives blue color after spraying with anisaldehyde/sulfuric acid and heating. Positive ESI-MS m/z : 379.3 [M+H-H₂O]⁺. $^1\text{H NMR}$ (400 MHz, CDCl_3 -d) δ_{H} 5.59 (1H, d, $J = 3.2$ Hz, H-6), 5.41 (1H, d, $J = 2.0$ Hz, H-7), 5.28-5.16 (2H, m, H-22, H-23), 3.69-3.63 (1H, m, H-3), 2.49 (1H, d, $J = 16.7$ Hz, H-4a), 2.30 (1H, t, $J = 13.2$ Hz, H-4b), 2.09-1.85 (5H, m, CH_2 -2, H-9, H-16a, H-17), 1.28 (2H, s, CH_2 -12), 1.07 (3H, d, $J = 6.8$ Hz, CH_3 -21), 0.96 (3H, s, CH_3 -19), 0.94 (3H, d, $J = 6.8$ Hz, CH_3 -28), 0.89 (3H, d, $J = 6.0$ Hz, CH_3 -27), 0.85 (3H, d, $J = 6.4$ Hz, CH_3 -26), 0.65 (3H, s, CH_3 -18). $^{13}\text{C NMR}$ (CDCl_3 -d, 100 MHz), δ_{C} : 141.4 (C-8), 139.8 (C-5), 135.6 (C-23), 132.0 (C-22), 119.6 (C-6), 116.3 (C-7), 70.5 (C-3), 55.8 (C-17), 54.6 (C-14), 46.3 (C-9), 42.8 (C-13,24), 40.8 (C-4), 40.4 (C-20), 39.1 (C-12), 38.4 (C-1), 37.0 (C-10), 33.1 (C-25), 32.0 (C-2), 29.7 (C-16), 23.0 (C-15), 22.7 (C-11), 21.1 (C-21), 20.0 (C-27), 19.7 (C-26), 17.6 (C-19), 16.3 (C-28), 12.0 (C-18).

Compound 4: Yellow needles; R_f (0.14 (DCM)); yellow followed by grey color upon spraying with anisaldehyde/sulfuric acid reagent $^1\text{H NMR}$ (500 MHz, CDCl_3 -d) and $^{13}\text{C NMR}$ (125 MHz, CDCl_3 -d) data (table1); Positive ESI/MS: m/z : 347.1 [M+Na]⁺ and 671.1 [2M+Na]⁺ and negative ESI/MS: m/z : 322.9 [M-H]⁻.

Compound 5: Pale yellow oil, R_f (0.37, DCM/MeOH 95:5), it gives intense pink color on spraying with anisaldehyde/sulfuric acid reagent. UV (MeOH, λ_{max} , nm): 208, 278. Positive ESI/MS: m/z : 231.1102 [M+H]⁺ and negative ESI/MS: m/z : 229.1232 [M-H]⁻: $^1\text{H NMR}$ (500 MHz, CDCl_3 -d) δ_{H} 6.34 (4H, d, $J = 6.5$ Hz, 4/4', 6/6'); 6.23 (2H, t-like, $J = 2.0$ Hz, 2/2'); 4.68 (2H, s, 3/3' OH); 2.20 (6H, 7/7' CH₃). $^{13}\text{C NMR}$ (125 MHz, CDCl_3 -d), δ_{C} : 158.1 (C-1/1'), 156.5 (C-3/3'), 141.0 (C-5/5'), 112.1 (C-6/6'), 111.1 (C-4/4'), 103.5 (C-2/2'), 21.5 (C-7/7').

Compounds 6 and 9 were isolated as reddish-white needles with blue fluorescence under long UV light (360 nm). UV λ_{max} (MeOH) nm: 254.0; 338.0 (6) and 254.0, 292.0 336.0 (9). $^1\text{H NMR}$ (500 MHz for compounds 6 and 600 for 9, $(\text{CD}_3)_2$ -d₆) and $^{13}\text{C NMR}$ (150 MHz for 6 and 125 for 9, data are represented in table 2. Negative ESI-MS being m/z 270.9 and 256.8 for [M-H]⁻ of 6 and 9 respectively)

Compounds 7 and 8 were isolated as a mixture with a ratio 2:1 (based on the NMR data) and due to their small amount to be separated so they were identified in mixture form. The mixture was isolated as an orange powder and it gives orange fluorescence under long-UV (366 nm) light; UV (MeOH, λ_{max} , nm): 292, 450. Negative ESI mass showed m/z 367. 28 [M-H]⁻ for 7 and m/z 368.922 [M-2H]⁻ for 8. $^1\text{H NMR}$ (500 MHz, $(\text{CD}_3)_2$ -d₆) and $^{13}\text{C NMR}$ (125 MHz, $(\text{CD}_3)_2$ O-d₆) data are represented in (table 3).

Cytotoxicity assay

Cytotoxic activities were tested using Human Breast adenocarcinoma (MCF-7), Hepatocellular carcinoma cells (Hep G2),

and normal cell lines WI-38 using the microculture tetrazolium assay (MTT), and compared to that of untreated controls [12]. Cells were routinely cultured in Dulbecco's Minimum Essential Media (DMEM), which supplemented with 10% fetal bovine serum, 100 unit/ml penicillin, 100 units/ml streptomycin, and 250 ng/ml amphotericin B (Cambrex BioScience, Copenhagen, Denmark). Cells were maintained at sub-confluence at 37 °C in humidified air containing 5% CO₂. For sub-culturing, monolayer cells were harvested after trypsin/EDTA treatment at 37 °C. Cells were used when confluence had reached 75%. For cytotoxicity assay, cells (0.5X10⁵ cells/well), in serum-free medium, were seeded in 96-well microplate and treated with tested compounds and the extract (20 µl medium/well) at four concentrations (100, 50, 25 and 12.5 µg/ml in DMSO) then incubated for 24 h at 37 °C, in a humidified 5% CO₂ atmosphere. After incubation, media was removed and 40 µl MTT solution/well was added and incubated for an additional 4 h. MTT crystals were solubilized by the addition of 180 µl of DMSO to each well using a micropipette and left at room temperature for 45 s. The presence of viable cells was visualized by the development of purple color due to the formation of formazan crystals and then measuring the absorbance at 570 nm using a microplate ELISA reader. Triplicate repeats were performed for each concentration and the average was calculated. Data were expressed as a percentage of relative viability compared to the untreated cells and the vehicle control (DMSO), with cytotoxicity indicated by <100% relative viability. The half-maximal inhibitory concentration of viability (IC₅₀) was calculated from the equation of the dose-response curve.

Mode of cell death

To identify the mode of the anticancer activity of the compounds **4** and mixture of **7** and **8**, each cell line (1 x 10⁴ cells) was treated with 50 % of the IC₅₀ on cell culture slides (SPL, South Korea) for 24 h. The slides were washed with phosphate buffer saline (PBS) and stained with ethidium bromide/acridine orange (10 µl of 100 µg/ml of each in equal volume mix in 100 µl PBS) for 10 min. in the dark and then examined under a fluorescence microscope (Axio Imager

Z2, Zeiss, Germany). Percentage of living, apoptotic and necrotic cells were calculated for each sample concentration at its respective cell line.

Molecular docking study

The three-dimensional structures of the most active compounds (**7** and **8**) against MCF7 and hepatocellular and HeP G2 cell lines were done. **7** and **8** in their neutral forms were constructed using the MOE of Chemical Computing Group Inc software. The lowest energy conformer of both analogs "global-minima" was found by the conformational search. The protein structure of the heat shock protein enzyme with the code number of 1YET was taken from Protein Data Bank of Brookhaven National Laboratory and imported into MOE software [13]. Crystal structure of heat shock protein 90-geldanamycin (Hsp 90) complex: targeting of a protein chaperone by an anticancer agent. Protein preparation was carried out and it was energy minimized, all of the hydrogen atoms were added and the enzyme structure was subjected to refinement protocol imported in MOE followed by docking of most active conformers into the Hsp 90 enzyme-binding domain. The energy of binding was calculated. The docking was performed using the Alpha Triangle placement method and the London dG scoring method. 300 Results for each ligand were generated, discarding the results with an RMSD value>3 Å. The best-scored result of the remaining conformations for each ligand was further analyzed [14, 15].

RESULTS AND DISCUSSION

Chemistry

Chromatographic fractionation of the ethyl acetate extract of *Aspergillus* sp isolated from *M. subulata* leaves resulted in the identification of nine compounds (fig. 1), their structures were established using different physical and chemical methods. Compounds **1** and **3** were identified as methyl lineolate and ergosterol, respectively based on their spectroscopic data and comparison with authentic sample and published data [16-19].

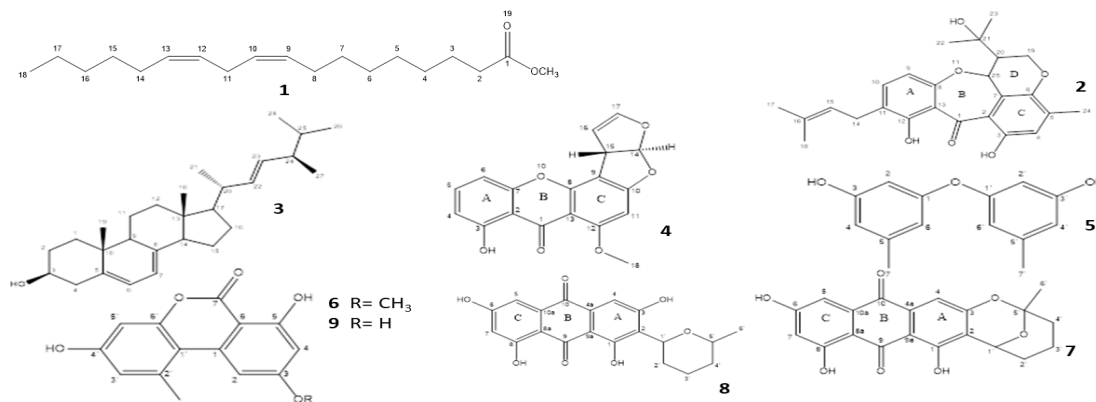


Fig. 1: Structures of the compounds identified from *Aspergillus* sp

Compound 2

Based on its chromatographic properties, it was expected that **2** is hydroxylated and/or methylated xanthones [20]. Its ¹H-NMR data (table 1) exhibited two characteristic singlet signals of the two exchangeable protons at δ_H 13.80 and 10.63 for OH-12 and 3, respectively. It also displayed three aromatic protons, two of which are *ortho* coupling at δ_H 6.34 (H-9) and 7.21 (H-10) and the third one as a singlet signal for H-4 (δ_H 6.74), which confirmed the presence of two aromatic rings (A, C). The presence of doublet signal at δ_H 3.24 (CH₂-14) together with multiplet one integrated for one proton at δ_H 5.25 (CH-15) in addition to the presence of two singlet signals each integrated for three protons at δ_H 1.69 and 1.65 for two methyl group at C-17 and 18 respectively gave evidence for the presence of

prenyl group in its structure. In addition to the ¹H NMR data (table 1) showed a doublet signal at δ_H 5.01 for sp³ oxygenated methine proton (H-25) and doublet triplet signal at δ_H 2.30 for non-oxygenated one (H-20) together with one sp³ methylene group at δ_H 4.30 and 4.12 (CH₂-19) which gave evidence for the presence of tetrahydropyran ring in the structure (D). Moreover, the three methyl groups at C-22, 23, and 24 were confirmed from the three singlet signals at δ_H 1.25, 1.19, and 2.17, respectively. HMQC with ¹³CNMR (table 1) confirms that all non-exchangeable proton resonances were associated with the directly attached carbon atoms. Analysis of the ¹H-¹H COSY and ¹H-¹³C HMBC (table 1) experiments and the coupling values of the protons of **2** indicated the correlation between H-9 (δ_H 6.34) and H-10 (δ_H 7.21) as well as in HMBC spectrum there is a correlation between H-9 and C-13 (112.6), C-

11(124.1), C-8 (159.1) and C-1 (197.2) besides the correlation between H-10 and C-8 (159.1), C-12 (163.4) and C-14 (27.7) which support the substitution pattern of the ring A. Moreover, the substitution pattern of the ring C is established from the correlation between H-4 (δ_H 6.74) and C-6 (145.3), C-3 (155.6), C-2 (119.7), C-1 (197.2), and C-24 (16.6). The presence of the prenyl group was confirmed from the correlation of CH₂-14 (δ_H 3.24) with H-15 (δ_H 5.25). HMBC spectrum confirmed this suggestion by the presence of the correlations between CH₂-14 (δ_H 3.24) with C-15 (121.8) and C-16 (133.3) and the correlation of CH₃-17 (1.69) and CH₃-18 (1.65) with C-15 (121.8) and C-16 (133.3). Its position was proven to be at C-11 of ring A by correlations between CH₂-14 and C-10 (137.7), C-11 (124.1), and C-12 (163.4). The presence of ring D was established from the correlation of H-19 (δ_H 4.12, 4.30) with each other, and with H-20 (δ_H 2.3) as well as H-20 was correlated with H-19 and H-

25 (δ_H 5.01). Moreover, ring D was confirmed from the HMBC in which H-19 (δ_H 4.12,4.30) is coupled with C-20 (49.3), C-6 (145.3), and C-25 (74.1); H-20 (δ_H 2.30) correlated with C-19 (65.2) and C-25 (74.1) as well as H-25 (δ_H 5.01) is correlated with C-19 (65.2), C-20 (49.4), C-6 (145.3), C-7(120.6) and C-8 (159.1). The presence of isopropyl group was confirmed from the HMBC where the correlation between CH₃-22 (δ_H 1.25) and 23 (δ_H 1.19) with C-21 (71.2) and its position was established from the correlation between CH₃-22 and 23 with C-20 and between H-25, H-20, and H-19 with C-21. The methyl group at C-5 was confirmed from the coupling of CH₃-24 with C-4 (120.2), C-5 (136.5), and C-6 (145.3). The carbonyl carbon was detected in ring B due to the correlation between H-9 and H-4 with C-1 (197.2). Finally, the positive ESI/Ms showed a base peak at 447.3 for [M+Na], which confirms the molecular formula C₂₅H₂₈NaO₆. Based on the above analyses **2** is identified as arugosin C [21, 22].

Table 1: ¹H NMR (500 MHz) and ¹³C NMR (125 MHz) in (CDCl₃-d) data for **2** and **4**

S. No.	2				4			
	δ_C	δ_H	¹ H- ¹ H COSY	HMBC	δ_C	δ_H	¹ H- ¹ H COSY	HMBC
1	197.2				181.4			
2	119.7				109.0			
3	155.6				162.3			
4	120.2	6.74 (s)		6, 3, 2, 1,24	111.3	6.69 (dd, 8.5, 1.0)	5	2,3,7,13
5	136.5				135.7	7.44 (t like, 8.0)	4,6	2,3,7
6	145.3				105.9	6.77 (dd, 7.0,1.0 overlapped with H-14)	5	1,2,4,7
7	120.6				155.0			
8	159.1				154.1			
9	108.9	6.34 (d, 8.5)	10	13,11,8,1	106.5			
10	137.7	7.21 (d, 8.5)	9	12,8,14	164.6			
11	124.1				90.5	6.38 (s)		1,8,9,13,10,12
12	163.4				163.3			
13	112.6				106.0			
14	27.7	3.24 (d, 7.5, CH ₂)	15	10,11,12,15,16	113.3	6.77 (d, 7.0)	15	9,10,15,16,17
15	121.8	5.25 (m)	14	18,17,14	48.1	4.75 (dt, 7.5, 2.5)	14,16	9,10,14,16,17
16	133.3				102.5	5.39 (t, 2.5,3.0)	15,17	14,15,17
17**	25.8	1.69(s, 3H)		15,16	145.4	6.44 (dd, 2.5, 2.0)	16	14,15,16
18**	17.8	1.65 (s, 3H)		15,16				
19a	65.2	4.30 (dd,11.5,4.0),	20	6,21,20,25				
19b		4.12 (dd, 11.5,7.0)						
20	49.4	2.30 (dt, 7, 4.00)	19,25	19,21,25				
21	71.2							
22	29.0	1.25(s, 3H)		20,21				
23	28.2	1.19(s, 3H)		20,21				
24	16.6	2.17 (s, 3H)		4,5,6				
25	74.1	5.01(d,4.5)	20	6,7,8,19,20,21				
12-OH		13.80 (s)		11,12,13				
3-OH		10.63 (s)		3,2,4,5		13.16		1,2,3,4,5
OCH ₃					56.8	3.93 (s)		11,12

*Data between parentheses represent the J value in Hz; ** H-17 and H-18 are exchangeable

Compound 4

As in the case of **2**, it was expected that compound **4** is related to hydroxylated and/or methoxylated xanthenes [20]. Its ¹H NMR data of **4** (table 1) showed a singlet signal at δ_H 13.16 for the hydrogen-bonded phenolic hydroxyl proton at C-3. The trisubstituted aromatic ring (A) was established from the presence of three signals at δ_H 6.69 (dd); 7.44 (t-like), and 6.77 (dd), in addition to the presence of a singlet signal at δ_H 6.38 for H-11 revealed the presence Penta substituted aromatic ring (B). The presence of rings A and B confirmed that **4** is related to hydroxylated and/or methoxylated xanthenes. Moreover, the presence of four proton signals at δ_H 6.77 (d H-14), 4.75 (dt, H-15), 5.39 (t like H-16), and 6.44 (dd, H-17) and singlet signal at δ_H 3.93 gave evidence for the presence of furan ring and methoxy group respectively. ¹³C NMR spectrum (table 1) showed thirteen carbon resonances characteristic for xanthone nucleus with the key signal of carbonyl carbon at δ_C 181.4 [23, 24] in addition to the methoxy group at δ_C 56.8 and another four carbons of the furan ring. ¹H-¹H COSY data (table1) confirmed the presence ring

A by the presence of a correlation between H-5 (δ_H 7.44) with H-4 (δ_H 6.69) and H-6 (δ_H 6.77) and it was further established from the HMBC (table 1) by the correlation between H-4 (δ_H 6.69) and C-2 (109.0), C-3 (162.3) and C-7 (155.0), also between H-5 (δ_H 7.44) and C-3 (162.3) and C-7(155), in addition to the correlation between H-6 (δ_H 6.77) and C-1 (181.4), C-2 (109.0), C-4 (111.3), and C-7 (155.0). The presence of ring B was confirmed by the presence of a correlation between H-11(δ 6.38) and C-12 (163.3), C-13 (106.0), C-1 (181.4), C-8 (154.0), C-9 (106.5), and C-10 (164.6) in HMBC. Moreover, the correlations of CH₃-18 (δ_H 3.93) with C-11 (90.5) and C-12 (163.3) gave evidence for the presence of the methoxy group attached at C-12. The presence of bisfuranic ring was established from ¹H-¹H COSY through the correlation between H-15 (δ_H 4.75), H-14 (δ_H 6.77) and H-16 (δ_H 5.39) as well as the correlation of H-16 (δ_H 5.39) with H-15 (δ_H 4.75) and H-17 (δ_H 6.44) and further confirmed from HMBC which showed a correlation between H-14 (δ 6.77) and C-9 (106.5), C-10 (164.6), C-15 (48.1), C-16 (102.5) and C-17 (145.4) as well as the correlation between H-15 (δ_H 4.75) and C-9 (106.5), C-10 (164.6), C-14 (113.3), C-17 (145.4) and C-16 (102.5), in addition

to the correlation between H-17 and C-14, C-15 and C-16. The presence of OH-3 was established from the correlation between OH-3 and C-1, C-2, C-3, C-4 and C-5 in the HMBC. The above interpretation for the structure of **4** was finally positive ESI/MS, which showed a molecular ion peak at m/z 347.1, for a molecular formula $C_{18}H_{12}O_6$ Na. Therefore it was identified as sterigmatocystin [23, 24].

Compound 5 exhibits chromatographic properties and UV data that resemble a simple aromatic compound [25]. Its 1H NMR showed a doublet signal integrated for four *meta* coupled protons at δ_H 6.34 (4/4', 6/6') and t-like signal integrated for two *meta* coupled protons δ_H 6.23 (2/2'), which is an indication that **5** may be identical molecules linked together. Moreover, the singlet signal at δ_H 2.20 for 7/7' CH_3 which was integrated for 6 H and another one at δ_H 4.68 for two protons of phenolic OH-3/3' confirmed this suggestion. ^{13}C NMR data and HSQC data showed that compound **5** has six CH group and quaternary carbons in the aromatic region in addition to two methyl groups. Positive and negative ESI/MS showed m/z at 231.1102 [M+H]⁺ and 229.1232 [M-H]⁻ respectively together with 1H - 1H COSY and HMBC data establish that compound **5** is a dimer of 3-hydroxyl, 5-methyl phenyl ether and identified as 3, 3'-dihydroxy-5, 5'-dimethyl diphenyl ether (diorcinol) [25].

Compounds 6 and 9

They gave physical and UV data typical to the pattern of coumarin compounds like alternariol [26]. 1H NMR data of them (table 2) showed the presence of four *meta*-coupling doublets each integrated

for one proton (δ_H 6.44 to 7.18) and (δ_H 6.46 to 7.37) respectively indicated the presence of two tetrasubstituted aromatic rings. In addition to the presence of singlet signals at $\delta_H \approx 2.7$ integrated for three protons gave evidence for the presence of methyl groups attached to an aromatic ring. Moreover, the presence of a singlet signal at δ_H 3.85 in **6** indicated to the presence of additional methoxy in its structure, which confirmed from the [M-H]⁻ of **6** at m/z 270.9 with an increase of 14 mass units compared to **9** (m/z 256.8). The singlet signal at $\delta_H \approx 11.85$ is indicative of the presence of a chelated hydroxyl group. ^{13}C NMR data of both compounds (table 2) revealed the presence of 14 carbons atoms among which a signal at δ_C (165.2) indicated the presence of a conjugated lactone (C-7) characteristic for coumarin structure together with signal $\approx \delta_C$ 24.7 for methyl group, besides, to signal at δ_C 55.4 for methoxy group in **6**. Further confirmation of the two compounds was achieved by HMBC spectrum (table 2), which showed the correlations of the *meta*-coupled protons, H-4 to C-2, C-3, C-5, and C-6 as well as H-6 to C-2, C-4, C-5, and 1' which established the structure of the first aromatic ring. Moreover, the second aromatic ring was confirmed from the correlation H-3' with C-1', C-2', C-4', and 5' as well as H-5' to C-1', C-3' and 6'- CH_3 . The position of CH_3 at C-6' was proved from the correlations of the aromatic methyl group to C-1, C-1', C-5', C-6' and C-6'. Furthermore, the correlation of the OCH_3 group to C-5 in compound **6** was indicative of its position. Moreover, correlations of the methyl group to C-6' and correlation of H-6 to C-1' proved the point of attachment of both aromatic rings. Based on the above data, compound **6** is identified as alternariol-5-*O*-methyl ether and **9** is alternariol [26-28].

Table 2: 1H and ^{13}C -NMR in [(CD₃)₂-d₆] data for **6**(500, 125 MHz) and **9**(600,150 MHz)

Carbon	6		HMBC for 6/9	9	
	δ_C	δ_H		δ_C	δ_H
1	138.2			138.6	
2	98.9**			98.3	
3	165.1			165.1	
4	98.0**	6.44 (1H, d, 2.0)	2,3,5,6 (6); 2,3,6(9)	101.0	6.46 (1H, d, 1.8)
5	166.7			165.1	
6	103.7	7.18 (1H, d, 2.0)	2, 4, 5, 1' (6); 2,3,4,1' (9)	104.3	7.37 (1H, d, 1.2)
7	165.2			165.1	
1'	109.7			109.8	
2'	153.2			153.2	
3'	101.9	6.58 (1H, d, 2.5)	1', 2', 4', 5' (6); 1', 2',5' (9)	101.8	6.70 (1H, d, 2.4)
4'	158.5			158.1	
5'	117.6	6.68 (1H, d, 2.5)	1', 3', 6'- CH_3	117.4	6.80 (1H, d, 2.4)
6'	138.8			138.7	
3-OH		11.85 (1H, s)	2,3,4		11.95 (1H, s)
5-O CH_3	55.4	3.85 (3H, s)	5	-	-
6'- CH_3	24.7	2.68 (3H, s)	1, 1', 5', 6',6	24.8	2.78 (3H, s)

The value between parentheses represents *J* value in Hz; * obtained from HMQC and HMBC experiments; ** Carbon value may be interchangeable

Compound 7 and 8

Based on the color of compounds **7** and **8** under long UV light and the UV absorbance at λ_{max} (MeOH) 292 and 450 nm, we suggested that the two compounds have a phenyl anthraquinone chromophore [29]. 1H NMR of **7** (table 3) displayed two singlet signals for hydrogen-bonded hydroxyl groups at δ_H 12.39 (OH-1) and 12.06 (OH-8). Moreover, it revealed the presence of three aromatic protons, two of which are *meta* doublets at δ_H 7.10 and 6.51 for H-5 and H-7 of the ring C and the other one at δ_H 6.98 for H-4 of the ring A. Besides it showed one methyl group at δ_H 1.41 (H-6'), one methine at δ_H 5.16 attached to an oxygen atom, and three methylene groups δ_H 1.69-1.73, 1.30-1.58; 1.74-1.94 (1H, m), for H-2', H-3' and H-4', respectively. ^{13}C NMR and DEPT (table 3) spectra showed 20 carbon signals, attributable to one methyl (δ_C 27.12), three methylene (δ_C 15.66, 27.17, 35.48), four methane (δ_C 66.63, 107.64, 108.12, 108.68), ten quaternary (δ_C 101.34, 108.76, 109.39, 116.31, 133.65, 135.53, 159.07, 160.68, 165.07, 165.17), and two ketone carbonyl (δ_C 180.84, 189.79) carbons which indicative for the presence quinone group. Based on the ^{13}C NMR together with 1H NMR and mass spectral data, the molecular formula of **7** is $C_{20}H_{16}O_7$,

which supported by m/z 368.928 [M-H]⁻. The assignments of the protons and carbons signals were accomplished by a further analysis of the 1H - 1H COSY and HMBC data, which confirmed the configuration of the ring C through the correlation between H-5 and H-7 as well as its correlation with C-6, C-10, and C-8a and the correlation between H-7 with C-8, C-8a. Furthermore, H-4 in ring A is correlated with C-10, C-2, and C-3. The presence of the methine group attached to the oxygen atom (δ_H 5.16, H-1') as well as its position, was confirmed from the correlation between H-1' and C-2, C-3, C-3', C-5' and C-2' in HMBC. Moreover, the correlation between the CH_3 -6' and C-1', C-4', C-5', C-3 gave evidence for its position. The presence of the remaining three methylene groups (H-2', H-3' and H-4') was established from the 1H - 1H COSY and HMBC (table 3). Therefore compound **7** was identified as averufin. [30-33]. As in the case of **7**, compound **8** showed two singlet signals for hydrogen-bonded hydroxyl groups and the signals characteristic for anthraquinones nucleus (table 3). Moreover, a doublet signal at δ_H 1.19 (CH_3 -6'), two methines at δ_H 5.01 (dd, *J* = 11.0, 2.5, H-1') and δ_H 3.69 (m, H-5') attached to an oxygen atom and three methylene groups for H-2', H-3' and H-4' gave evidence for the presence of another 5-methyl pyran ring in the structure. ^{13}C NMR and DEPT spectra (table

3) establish the presence of a quinine group. Besides, it confirmed the presence of the pyran ring by displaying the two carbon signals at δ_c 76.01 and 75.78 characteristics for two methane carbons at C-1' and C-5' respectively, and three methylene groups at (δ_c 30.0, 23.0, 32.6 for C-2', C-3' and C-4' respectively). Furthermore, the presence of a carbon

signal at δ_c 21.26 gave evidence for the presence of one methyl group at C-6'. Based on the ^{13}C NMR together with ^1H NMR and mass spectral data, the molecular formula of **8** is $\text{C}_{20}\text{H}_{18}\text{O}_7$. ^1H - ^1H COSY and HMBC (table 3) together with a comparison with reference data confirmed the structure as averufanin [30, 32, 33].

Table 3: ^1H (500 MHz) and ^{13}C -NMR (125 MHz) in (CDCl_3 -d) data for **7** and **8**

S. No.	7				8			
	δ_c	δ_H	^1H - ^1H COSY	HMBC	δ_c	δ_H	^1H - ^1H COSY	HMBC
1	159.1				160.8			
2	116.3				119.5			
3	160.7				163.2			
4	107.6	6.98(1H, s)		10, 2, 3	109.6	6.96(1H, s)		2,10
5	108.7	7.10 (1H, d, 2.5)	7	6, 10,8a	108.7	7.10(1H, d, 2.5)	7	6, 10, 8a
6	165.1				165.1			
7	108.1	6.51 (1H, d,2.0)	5	8, 8a	108.1	6.51(1H, d, 2.0)	5	8, 8a
8	165.2				165.2			
9	189.8				189.9			
10	180.8				180.9			
10a	135.5				135.5			
8a	109.4				109.4			
9a	108.8				108.7			
4a	133.7				133.7			
1'	66.6	5.16(1H,d, 3.0)	2'	2, 3, 3', 5',2'	76.0	5.01 (1H, dd, 11.0, 2.5)	2''	2, 3
2'	27.2	1.69-1.73 (2H, m)	1', 3'	3', 4', 5'	30.0	1.45-1.94 (2H, m)	1', 3'	Not detected
3'	15.7	1.30-1.58 (2H, m)	2', 4'		23.0	1.83 (2H, m)	2', 4'	5'
4'	35.5	1.74-1.94 (2H, m)	3'	1', 3', 2', 5'	32.6	1.2-1.67 (2H, m)	3', 5'	2'
5'	101.3		-		75.8	3.69 (1H, m)	4'	
6'	27.1	1.41(3H, s)		4', 5', 3, 1'	21.3	1.19 (3H, d,6.5)		4', 5'
1-OH		12.39(1H, s)		1, 2, 9a		12.42(1H, s)		1, 2, 9a
8-OH		12.06		8, 7		12.04(s)		8, 7

*Data between parentheses represent the J value in Hz; **H-17 and H-18 are exchangeable

Cytotoxic activity

Cytotoxic activity of the tested compounds and the ethyl acetate extract on both tested cell lines was expressed as IC_{50} in (table 4). A mixture of compounds **7** and **8** showed moderate cytotoxic activity in comparison

to other compounds against two cell lines with IC_{50} value 77.3 and 76.6 respectively, while compound **4** exhibited moderate activity against Hep G2 only (IC_{50} 86.6), as well as the ethyl acetate extract, exerted moderate activity against MCF-7 cell line (IC_{50} 84.0) Compound **2**, **4** and **5** showed weak cytotoxic activity against both cell lines.

Table 4: Cytotoxic activity of the ethyl acetate extract and identified compounds

Compound/extract	IC_{50} ($\mu\text{g}/\text{ml}$)	
	MCF-7	Hep G2
Ethyl acetate extract	84.0	115.0
2	191.0	296.0
4	131.0	86.8
5	133.0	149.0
6	347.0	>2000
7, 8	77.3	76.6
9	>2000	240.0

Compound **4** and the mixture of **7** and **8** did not manifest necrotic and apoptotic cell death in the case of MCF-7 (10-35%) (fig. 2) while in the case of Hep G2, compound **4** caused apoptotic and necrotic cell death with 60 and 20 % respectively

while in case of a mixture of **7** and **8** being 40 and 15 (fig. 2). This finding suggests that the decrease in the number of Hep G2 cells using these compounds was due to apoptotic and necrotic processes.

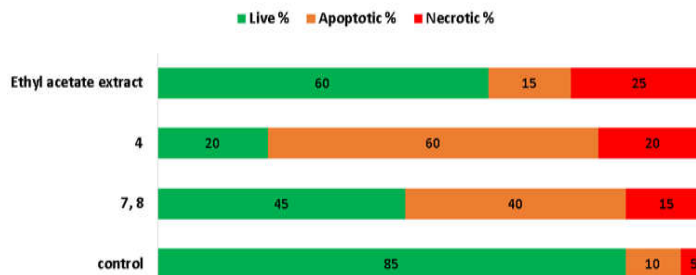


Fig. 2: Mode of cell death in MCF-7

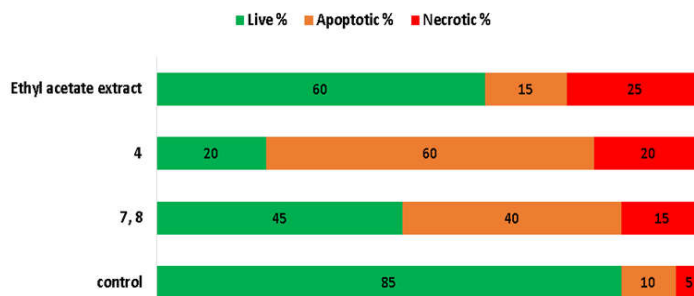


Fig. 3: Mode of cell death in Hep G-2

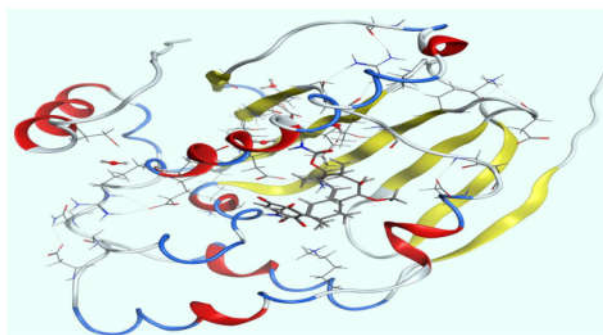


Fig. 4: 3D view of Hsp90 protein incorporated with reference inhibitor geldanamycin ligand in the crystal structure of human Hsp 90 (1YET.pdb) using MOE

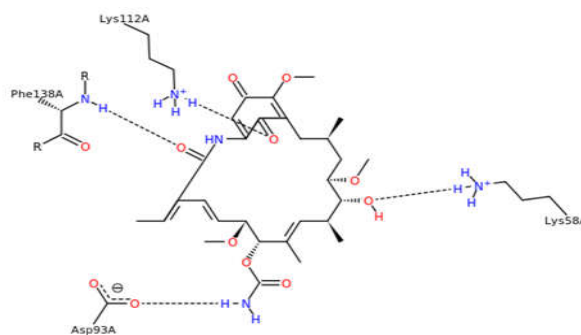


Fig. 5: 2D binding mode and residues for reference ligand geldanamycin active site of Hsp 90

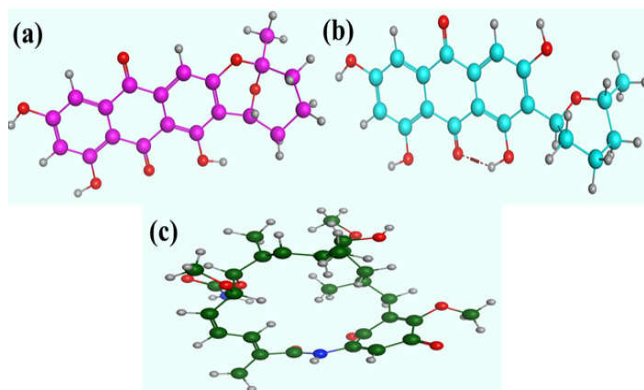


Fig. 6: Lowest energy conformers of (a) compound 7, (b) compound 8 and (c) geldanamycin reference, with balls and cylinders

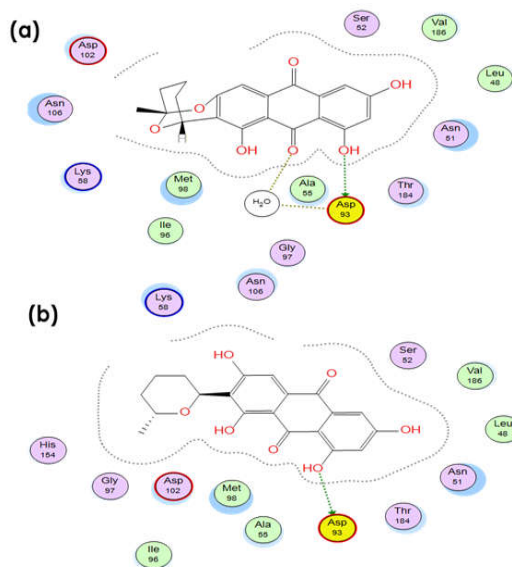


Fig. 7: 2D binding mode and residues involved in recognition of (a), compound 7 and (b) compound 8 into the ATPase site of Hsp 90 enzyme

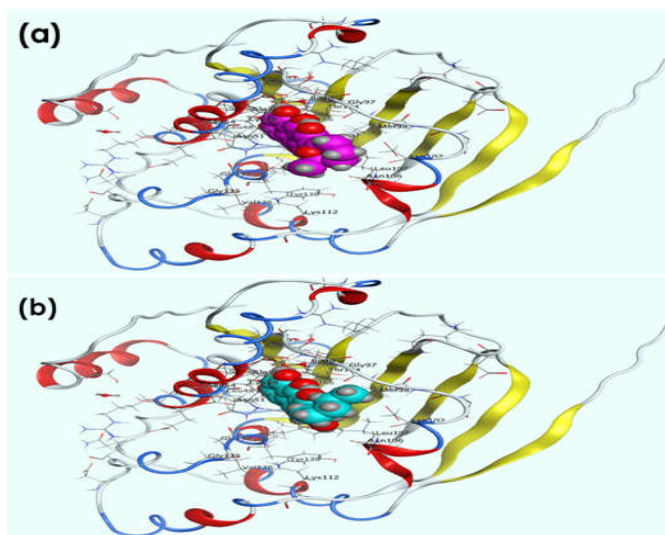


Fig. 8: The aligned conformations of active compounds (a) compound 7 and (b) compound 8 occupying the active site cavity of Hsp 90 enzyme

Molecular docking study

To suggest a mechanism of action of the compounds **7** and **8**, they were subjected to a molecular docking study in comparison to geldanamycin (a natural reference product of Hsp 90 inhibitor) (fig. 4). Important amino acids that were incorporated into the binding of geldanamycin into Hsp 90 enzyme were represented in fig. 5 and found to be composed of asp 93A, phe138A, Lys 112A, and lys 58A, hydrogen bonding interactions were found to be of great importance in binding. The lowest energy conformers of compounds under concern were represented in fig. 6. Molecular docking study indicated that **7** had recognition sites *via* hydrogen bonding network with the key amino acid asp 93 fig. 7a with a binding energy of -11.7561 Kcal/mol. Compounds **8** showed a bond acceptor interaction with asp 93 with a binding energy of -12.9432 Kcal/mol (fig. 7b). Fig. 8 clearly showed that both ligands **7** and **8** docked and buried in the active site showing that hydrogen bonding interactions

were representing an extremely important factor in binding with the enzyme. Therefore **7** and **8** were suggested to have their anticancer activity *via* Hsp 90 inhibition.

Cancer is one reason for death worldwide and according to the WHO (2004), about 12.5% of the population can die by cancer. It is characterized by the uncontrolled growth of abnormal cells which attacks the normal tissues; moreover, the cancer cells can also spread to other body parts to produce new tumors and which can lead to death if the spread of cells becomes uncontrolled [35]. Breast cancer is considered as one of the four major cancer types; it represents the highest incidence rate and is the second-highest cause of death in females [36]. Moreover, liver cancer or hepatic cancer represents the sixth most frequent cancer and is the second leading cause of death [37]. The main difficulty in the fight against cancer is the limited specificity of available chemical treatments, which lead the researchers to seek the isolation and screening of

natural compounds that can effectively target cancer cells without causing undesirable adverse side effects on normal cells. In recent years endophytic microorganisms have been considered a promising source of new drugs. Endophytic microorganisms are symbiotically associated, which causes indistinct symptoms, as well as they, have been recognized as a rich source of bioactive secondary metabolites [38]. Vincristine, vinblastine, taxol, and bleomycin are examples for currently used anticancer agents that have been isolated from endophytes and used in the treatment of different forms of cancers [39]. Sterigmatocystin (**4**) is structurally similar to mycotoxin with a bisdihydrofuran moiety and it has similar toxicity to Aflatoxin B1 and it is widely distributed in many endophytes and cereal grains of corn [40]. It can inhibit ATP synthesis and impair cell cycle also, it is considered to be a carcinogenic agent [40], as well as it forms an adduct of 1,2-dihydro-2-(N(7)-guanyl)-1-hydroxysterigmatocystin through its reaction with DNA in an Exo-ST-1,2-oxide structural form [41]. Due to the hepatocarcinogenic property of **4**, the human hepatoma Hep G2 cell was used as the cell model to investigate their cytotoxicity. It was reported that the low water solubility of **4** is considered the reason for its cytotoxicity since the low water solubility makes it easy to diffuse into the cells [40]. Anthraquinone compounds as compounds **7** and **8** have long been used as effective anticancer drugs. Based on their chemical skeletons, anthraquinone drugs can kill tumor cells through different mechanisms, involving different initial intracellular targets that normally contribute to drug-induced toxicity [42]. Both tested anthraquinone compounds contain basic planer skeleton, which represents the major contributor to the cytotoxicity properties, it was reported that the planar tricyclic structure of anthraquinone is essential for their cytotoxic activities and has been widely investigated for cancer therapy [43]. Previous researchers found that the position but not the number of the hydroxyl group in anthraquinone structure played an important role in determining its toxicity against normal and cancerous cell lines since they increase their solubility and might facilitate absorption or diffusion across the cellular membrane. Moreover, the polycyclic structure of anthraquinone can intercalate with DNA in between base pairs, either covalently or electrostatically, which possibly inhibits the DNA replication in cancer cell lines [44]. Hsp 90 enzyme has been implicated in a variety of disease states importantly in cancer, in which the chaperoning of mutated and overexpressed oncoproteins was critical. Inhibition of Hsp 90 leads to the degradation of multiple key proteins that depend on the interaction with Hsp 90 for maintaining their bioactive conformation. Targeting multiple oncogenic proteins provides an advantage for cancer therapy due to the potential to increase the therapeutic efficacy and to overcome the drug resistance that occurs in many cancer types, including our concerned ones; hepatic cancer and breast cancer. So, Hsp 90 was chosen to be our target for the anticancer mechanism of our active compounds.

This study reinforced the hypothesis that endophytes isolated from medicinal plants play an important role in the search for anticancer compounds. The observations from our study encourage further investigation on these plants.

CONCLUSION

Ethyl acetate extract of the rice culture of the *Aspergillus* sp isolated from *M. subulata* leaves showed the presence of different secondary metabolites, such as xanthenes, coumarins, and anthraquinones. The extract and some of the pure compounds showed cytotoxic activity against MCF-7 and Hep G2 cell lines with different strengths. Moreover, the strongest compound exhibited its activity through the apoptotic and necrotic process as well as binding to the effective site as in the case of geldanamycin.

FUNDING

This research did not receive any specific grant from funding agencies in the public, commercial, or not-for-profit sectors.

ACKNOWLEDGMENT

The authors are grateful to Dr. Ahmed S. Abdel-Razek, Microbial Chemistry Department, Genetic Engineering and Biotechnology Research Division, National Research Centre, Dokki-Giza, Egypt for

isolation of the *Aspergillus* sp. and departments of Organic and Bioorganic Chemistry, Faculty of Chemistry, Bielefeld University, Bielefeld, Germany for measuring spectroscopic data.

FUNDING

Nil

AUTHORS CONTRIBUTIONS

Reem AK: Isolate the compounds; Fatma AM: Identify the compounds and write the manuscript; Reham RI and Haitham AI: help in the identification of compounds and revise the manuscript; Shahenda ME: Carrying docking study.

CONFLICT OF INTERESTS

The authors declare that they have no competing interests.

REFERENCES

- Chang HS, Lin CH, Chen YS, Wang HC, Chan HY, Hsieh SY, *et al.* Secondary metabolites of the endophytic fungus *Lachnum abnorme* from *Ardisia cornudentata*. Int J Mol Sci 2016;17:1512.
- da Silva Ribeiro A, Polonio JC, Costa AT, Dos Santos CM, Rhoden SA, Azevedo JL, *et al.* Bioprospection of culturable endophytic fungi associated with the ornamental plant *Pachystachys lutea*. Curr Microbiol 2018;75:588-96.
- Kusari S, Singh S, Jayabaskaran C. Rethinking production of taxol(R) (paclitaxel) using endophyte biotechnology. Trends Biotechnol 2014;32:304-11.
- Wang XJ, Min CL, Ge M, Zuo RH. An endophytic sanguinarine-producing fungus from *Macleaya cordata*, *Fusarium proliferatum* BLH51. Curr Microbiol 2014;68:336-41.
- Pan F, Su TJ, Cai SM, Wu W. Fungal endophyte-derived *Fritillaria unibracteata* var. wabuensis: diversity, antioxidant capacities *in vitro* and relations to phenolic, flavonoid or saponin compounds. Sci Rep 2017;7:42008.
- Frisvad JC, Larsen TO. Chemodiversity in the genus *Aspergillus*. Appl Microbiol Biotechnol 2015;99:7859-77.
- Bladt TT, Frisvad JC, Knudsen PB, Larsen TO. Anticancer and antifungal compounds from *Aspergillus*, *Penicillium*, and other filamentous fungi. Molecules 2013;18:11338-76.
- Zhang H, Tang Y, Ruan C, Bai X. Bioactive secondary metabolites from the endophytic *Aspergillus* genus. Rec Nat Prod 2016;10:1-16.
- Li ZX, Wang XF, Ren GW, Yuan XL, Deng N, Ji GX, *et al.* Prenylated diphenyl ethers from the marine algal-derived endophytic fungus *Aspergillus tennesseensis*. Molecules 2018;23:2368.
- Vadlapudi V, Borah N, Yellusani KR, Gade S, Reddy P, Rajamanikyam M, *et al.* Aspergillus secondary metabolite database, a resource to understand the secondary metabolome of *Aspergillus* genus. Sci Rep 2017;7:7325.
- Innis MA, Gelfand DH, Sninsky JJ, White TJ. PCR protocols: a guide to methods and applications: Academic Press; 2012.
- James J, Thomas J. Anticancer activity of microalgae extract on human cancer cell line (mg-63). Asian J Pharm Clin Res 2019;12:139-42.
- Stebbins CE, Russo AA, Schneider C, Rosen N, Hartl FU, Pavletich NP. Crystal structure of an Hsp 90-geldanamycin complex: targeting of a protein chaperone by an antitumor agent. Cell 1997;89:239-50.
- Allinger NL. Conformational analysis. 130. MM2. A hydrocarbon force field utilizing V1 and V2 torsional terms. J Am Chem Soc 1977;99:8127-34.
- Profeta Jr S, Allinger N. Molecular mechanics calculations on aliphatic amines. J Am Chem Soc 1985;107:1907-18.
- Diaz MF, Gavin JA. Characterization by NMR of ozonized methyl linoleate. J Brazil Chem Soc 2007;18:513-8.
- Shirane N, Takenaka H, Ueda K, Hashimoto Y, Katoh K, Ishii H. Sterol analysis of DMI-resistant and -sensitive strains of *Venturia inaequalis*. Phytochemistry 1996;41:1301-8.
- Martinez M, Alvarez ST, Campi MG, Bravo JA, Vila JL. Ergosterol from the mushroom *Laetiporus* sp.: isolation and structural characterization. Rev Bol Quim 2015;32:90-4.
- Nowak R, Drozd M, Mendyk E, Lemieszek M, Krakowiak O, Kisiel W, *et al.* A new method for the isolation of ergosterol and

- peroxyergosterol as active compounds of *Hygrophoropsis aurantiaca* and *in vitro* antiproliferative activity of isolated ergosterol peroxide. *Molecules* 2016;21:946.
20. Davies J, Kirkaldy D, Roberts JC. 437 Studies in mycological chemistry. Part VII. Sterigmatocystin, a metabolite of *Aspergillus versicolor* (Vuillemin) tiraboschi. *J Chem Soc* 1960;0:2169-78.
 21. Ballantine JA, Ferrito V, Hassall CH, Jenkins ML. The biosynthesis of phenols. Part XXIV. Arugosin C, a metabolite of a mutant strain of *Aspergillus rugulosus*. *J Chem Soc Perkin Trans* 1973;1:1825-30.
 22. Hawas UW, El-Beih AA, El-Halawany AM. Bioactive anthraquinones from endophytic fungus *Aspergillus versicolor* isolated from red sea algae. *Arch Pharm Res* 2012;35:1749-56.
 23. Zhu F, Lin Y. Three xanthenes from a marine-derived mangrove endophytic fungus. *Chem Nat Compd* 2007;43:132-5.
 24. Pachler KG, Steyn PS, Vleggaar R, Wessels PL. Carbon-13 nuclear magnetic resonance assignments and biosynthesis of aflatoxin B1 and sterigmatocystin. *J Chem Soc Perkin* 1976;1:1182-9.
 25. Itabashi T, Nozawa K, Nakajima S, Kawai KI. A new azaphilone, falconensin H, from *Emericella falconensis*. *Chem Pharm Bull* 1993;41:2040-1.
 26. Hassan A. Novel natural products from endophytic fungi of Egyptian medicinal plants-chemical and biological characterization [Dissertation]. Düsseldorf: Universität Düsseldorf; 2007.
 27. De Souza GD, Mithofer A, Daolio C, Schneider B, Rodrigues-Filho E. Identification of *Alternaria alternata* mycotoxins by LC-SPE-NMR and their cytotoxic effects to soybean (*Glycine max*) cell suspension culture. *Molecules* 2013;18:2528-38.
 28. Tan N, Tao Y, Pan J, Wang S, Xu F, She Z, *et al.* Isolation, structure elucidation, and mutagenicity of four alternariol derivatives produced by the mangrove endophytic fungus No. 2240. *Chem Nat Compd* 2008;44:296-300.
 29. Dagne E, Yenesew A, Asmellash S, Demissew S, Mavi S. Anthraquinones, pre-anthraquinones, and isoeleutherol in the roots of *Aloe* species. *Phytochemistry* 1994;35:401-6.
 30. Chen M, Shao C-L, Kong C-J, She Z-G, Wang C-Y. A new anthraquinone derivative from a gorgonian-derived fungus *Aspergillus* sp. *Chem Nat Compd* 2014;50:617-20.
 31. Cole RJ, Cox RH. *Handbook of toxic fungal metabolites*: Academic Press; 1981.
 32. Gorst-Allman CP, Pachler KG, Steyn PS, Wessels PL. Carbon-13 nuclear magnetic resonance assignments of some fungal C 20 anthraquinones; their biosynthesis in relation to that of aflatoxin B 1. *J Chem Soc Perkin* 1977:2181-88.
 33. Shao C, Wang C, Wei M, Li S, She Z, Gu Y, *et al.* Structural and spectral assignments of six anthraquinone derivatives from the mangrove fungus (ZSUH-36). *Magn Reson Chem* 2008;46:886-9.
 34. Özkaya FC, Ebrahim W, El-Neketi M, Tanrıkul TT, Kalscheuer R, Müller WE, *et al.* Induction of new metabolites from the sponge-associated fungus *Aspergillus carneus* by OSMAC approach. *Fitoterapia* 2018,131:9-14.
 35. Metha SD, Paliwal S. Phytochemical analysis, liquid chromatography, and mass spectroscopy and *in vitro* anticancer activity of *Annona squamosa* seeds lin. *Asian J Pharm Clin Res* 2018;11:101-3.
 36. Examination IN, Wulandari A, Putihuspa DH, Andayaningsih P. Cytotoxicity of an aromatic compound from an endophytic fungus, *Cladosporium* sp. En-s01. *Int J Curr Pharm Res* 2018;10:10-12
 37. McGuire S. World cancer report 2014. Geneva, Switzerland: World Health Organization, the international agency for research on cancer, WHO Press, 2015. In: Oxford University Press; 2016.
 38. Suja M, Vasuki S, Sajitha N. Anticancer activity of compounds isolated from marine endophytic fungus *Aspergillus terreus*. *World J Pharm Pharm Sci* 2014;3:661-72.
 39. Zhivotovsky B, Joseph B, Orrenius S. Tumor radiosensitivity, and apoptosis. *Exp Cell Res* 1999;248:10-7.
 40. Liu Y, Du M, Zhang G. Proapoptotic activity of aflatoxin B1 and sterigmatocystin in HepG2 cells. *Toxicol Rep* 2014;1:1076-86.
 41. Essigmann J, Barker L, Fowler K, Francisco M, Reinhold V, Wogan G. Sterigmatocystin-DNA interactions: Identification of a major adduct formed after metabolic activation *in vitro*. *Proc Natl Acad Sci* 1979;76:179-83.
 42. Akhtar MN, Zareen S, Yeap SK, Ho WY, Lo KM, Hasan A, *et al.* Total synthesis, cytotoxic effects of damnacanthal, nordamnacanthal and related anthraquinone analogs. *Molecules* 2013;18:10042-55.
 43. Hsin LW, Wang HP, Kao PH, Lee O, Chen WR, Chen HW, *et al.* Synthesis, DNA binding, and cytotoxicity of 1, 4-bis (2-aminoethyl amino) anthraquinone-amino acid conjugates. *Bioorg Med Chem* 2008;16:1006-14.
 44. Pors K, Paniwnyk Z, Teesdale Spittle P, Plumb JA, Willmore E, Austin CA, *et al.* Alchemix: a novel alkylating anthraquinone with potent activity against anthracycline-and cisplatin-resistant ovarian cancer. *Mol Cancer Ther* 2003;2:607-10.